

# Dynamically Iterated Filters

A unified framework for improved iterated filtering via smoothing

Anton Kullberg, Martin A. Skoglund, Isaac Skog, *Senior Member, IEEE*, Gustaf Hendeby, *Senior Member, IEEE*

**Abstract**—Typical iterated filters, such as the *iterated extended Kalman filter* (IEKF), *iterated unscented Kalman filter* (IUKF), and *iterated posterior linearization filter* (IPLF), have been developed to improve the linearization point (or density) of the likelihood linearization in the well-known *extended Kalman filter* (EKF) and *unscented Kalman filter* (UKF). A shortcoming of typical iterated filters is that they do not treat the linearization of the transition model of the system. To remedy this shortcoming, we introduce *dynamically iterated filters* (DIFs), a unified framework for iterated linearization-based nonlinear filters that deals with nonlinearities in both the transition model and the likelihood, thereby constituting a generalization of the aforementioned iterated filters. We further establish a relationship between the general DIF and the approximate iterated Rauch-Tung-Striebel smoother. This relationship allows for a Gauss-Newton interpretation, which in turn enables explicit step-size correction, leading to damped versions of the DIFs. The developed algorithms, both damped and non-damped, are numerically demonstrated in three examples, showing superior mean-squared error as well as improved parameter tuning robustness as compared to the analogous standard iterated filters.

**Index Terms**—Nonlinear filtering, statistical linearization, Kalman filters, iterative methods

## I. INTRODUCTION

The problem of state estimation is ubiquitous and appears in a wide range of fields, such as engineering, robotics, economics, etc. This task requires a system model that describes the system's dynamical evolution as well as a measurement model that links observed quantities to the state of the system. The system model can be represented either functionally or probabilistically as a transition and measurement density. The two representations are given by

$$\begin{aligned} \mathbf{x}_{k+1} &= \mathbf{f}(\mathbf{x}_k, \mathbf{w}_k), \mathbf{w}_k \sim p(\mathbf{w}_k) && p(\mathbf{x}_{k+1}|\mathbf{x}_k) \\ \mathbf{y}_k &= \mathbf{h}(\mathbf{x}_k, \mathbf{e}_k), \mathbf{e}_k \sim p(\mathbf{e}_k) && \rightarrow p(\mathbf{y}_k|\mathbf{x}_k) \end{aligned} \quad (1)$$

Here,  $\mathbf{x}_k$ ,  $\mathbf{y}_k$ ,  $\mathbf{w}_k$ , and  $\mathbf{e}_k$  denote the state, the measurement, the process noise, and the measurement noise at time  $k$ , respectively. With this model, the state estimation problem involves computing either the smoothing posterior  $p(\mathbf{x}_{0:k}|\mathbf{y}_{1:k})$  or the filtering posterior  $p(\mathbf{x}_k|\mathbf{y}_{1:k})$ . If the model is affine with additive Gaussian noise, the most well-known filtering algorithm is the analytically tractable *Kalman filter* (KF), which is the

This work was partially supported by the Wallenberg AI, Autonomous Systems and Software Program (WASP) funded by the Knut and Alice Wallenberg Foundation.

A. Kullberg, M. A. Skoglund and G. Hendeby are with the Department of Electrical Engineering, Linköping University, Linköping SE-58183, Sweden (E-mail: {anton.kullberg, martin.skoglund, gustaf.hendeby}@liu.se).

I. Skog is with Uppsala University, Uppsala SE-75105, Sweden (E-mail: isaac.skog@angstrom.uu.se).

M. A. Skoglund is also affiliated with Eriksholm Research Center, Snekkersten, Denmark.

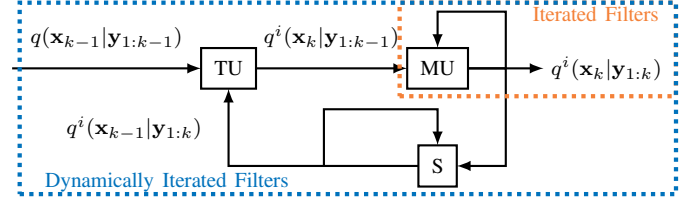


Fig. 1: Schematic illustration of a DIF. While standard iterated filters (dotted orange) only re-linearize the measurement update (MU), DIFs (dotted blue) also re-linearize the time update (TU) through a smoothing step (S). The smoothed distribution  $q^i(\mathbf{x}_{k-1}|\mathbf{y}_{1:k})$  is used to re-linearize the time update and smoothing step, whereas the current approximate posterior  $q^i(\mathbf{x}_k|\mathbf{y}_{1:k})$  is used for the measurement update. The steps are iterated until some convergence criterion is met.

optimal estimator in the *mean square error* (MSE) sense [1]. The smoothing analog is given by the *Kalman smoother* (KS), more specifically the *Rauch-Tung-Striebel* (RTS) smoother [2].

In many practical problems, a nonlinear system model is imperative to accurately capture the system's behavior. However, with these models, the state estimation problem becomes analytically intractable, now requiring approximate inference techniques. Consequently, a plethora of approximate filtering algorithms have been developed, including but not limited to the EKF, UKF, *cubature Kalman filter* (CKF), *particle filter* (PF), *point mass filter* (PMF), and many more [1], [3]–[7]. Similarly, smoothing analogs such as the *extended Kalman smoother* (EKS), *unscented Kalman smoother* (UKS), and *particle smoother* (PS) have also been developed [8]–[10]. In this paper, we focus on a family of methods that locally linearize the nonlinear model at each time step and subsequently utilize the KF recursions. This family encompasses not only the EKF but also various sigma-point filters, as these can be interpreted as methods that employ statistical linearization [11]. These methods include, among others, the UKF, the CKF, various sigma-point filters, and the Gaussian PF [3], [4], [12]–[16].

The linearization-based methods in focus here are generally computationally efficient and are in wide practical use, with the EKF being the *de facto* standard choice in many applications. However, linearization-based methods may suffer from convergence issues when the models are highly nonlinear. To remedy these convergence issues, iterative versions of these methods have been developed, such as the IEKF, the IUKF and the IPLF [17]–[25]. These iterative methods essentially perform multiple iterations of the measurement update in every filter update, each time re-linearizing the model around the current iterate, and can thereby improve the filter convergence and by extension the posterior approximation. Many of the methods have since been interpreted as *Gauss-Newton* (GN) methods, whereby further improvements have been proposed.

For instance, to improve local convergence properties, *damping* has been introduced, which is essentially a step-length correction based on some heuristic [26]–[30]. These damped methods have proven to be numerically efficient, often converge within a few iterations, and are broadly applicable to a wide range of problems.

However, previously proposed methods have focused their attention on nonlinearities in the measurement model (likelihood) and most often neglect any nonlinearities in the dynamical evolution of the system. For some cases, this is completely reasonable, as nonlinearities in the measurement model (likelihood) affect the posterior distribution to a greater extent than the transition model (prior). In other cases, this can lead to suboptimal performance or even divergence, as we show in our numerical experiments. To remedy this, in [31], we developed a unified scheme of so-called *dynamically iterated filters* (DIFs) that deal with the nonlinearities in both the measurement model (likelihood) *as well* as in the transition model (prior). The unified scheme encompasses both analytical and statistical linearization and thereby constitutes a generalization of the standard class of iterated linearization-based filters. In this paper, we further elaborate on this unified scheme and extend our prior work in multiple ways. Firstly, we provide a detailed connection between DIFs and iterated RTS smoothers, which allows us to interpret DIFs as GN algorithms. Secondly, in light of the GN connection, we introduce damping to further improve the local convergence properties of the DIFs. Lastly, we demonstrate the new family of methods on three numerical examples, each of which shows the benefits of the DIFs compared to their analogous iterated and non-iterated siblings.

The paper is organized as follows. In Section II, the general state estimation problem is formulated from a probabilistic viewpoint, and linearization-based methods are particularly discussed. Section III derives the DIFs, which closely follows our previous work [31]. In Section IV, the DIFs are interpreted as GN algorithms, and damped versions thereof are developed. Section V presents multiple examples where the DIFs, as well as their damped versions, are applied to different nonlinear systems. Lastly, Section VI discusses relevant connections to related work and outlines future research directions.

## II. PROBLEM FORMULATION

The general discrete-time state estimation problem is described here from a probabilistic point of view. We then describe linearization-based approaches in more detail and highlight their shortcomings.

### A. Discrete-time State Estimation

Consider a discrete-time *state space model* (SSM) given by

$$\mathbf{x}_{k+1} = \mathbf{f}(\mathbf{x}_k) + \mathbf{w}_k, \quad p(\mathbf{w}_k) = \mathcal{N}(\mathbf{w}_k; \mathbf{0}, \mathbf{Q}) \quad (2a)$$

$$\mathbf{y}_k = \mathbf{h}(\mathbf{x}_k) + \mathbf{e}_k, \quad p(\mathbf{e}_k) = \mathcal{N}(\mathbf{e}_k; \mathbf{0}, \mathbf{R}) \quad (2b)$$

We assume that  $\mathbf{x}_k \in \mathcal{X}, \forall k$  and that  $\mathbf{w}_k$  and  $\mathbf{e}_k$  are mutually independent. This can equivalently be expressed as

$$p(\mathbf{x}_{k+1}|\mathbf{x}_k) = \mathcal{N}(\mathbf{x}_{k+1}; \mathbf{f}(\mathbf{x}_k), \mathbf{Q}) \quad (3a)$$

$$p(\mathbf{y}_k|\mathbf{x}_k) = \mathcal{N}(\mathbf{y}_k; \mathbf{h}(\mathbf{x}_k), \mathbf{R}). \quad (3b)$$

Lastly, the initial state distribution is assumed to be given by

$$p(\mathbf{x}_0) = \mathcal{N}(\mathbf{x}_0; \hat{\mathbf{x}}_{0|0}, \mathbf{P}_{0|0}). \quad (4)$$

Now, given a sequence of measurements  $\mathbf{y}_{1:k} = \{\mathbf{y}_i\}_{i=1:k}$ , the smoothing problem involves computing the posterior of the state trajectory, *i.e.*,

$$p(\mathbf{x}_{0:k}|\mathbf{y}_{1:k}) = \frac{1}{\mathbf{Z}_{1:k}} p(\mathbf{x}_0) \prod_{i=1}^k p(\mathbf{y}_i|\mathbf{x}_i) p(\mathbf{x}_i|\mathbf{x}_{i-1}) \quad (5)$$

$$\mathbf{Z}_{1:k} \triangleq \int_{\mathcal{X}} p(\mathbf{x}_0) \prod_{i=1}^k p(\mathbf{y}_i|\mathbf{x}_i) p(\mathbf{x}_i|\mathbf{x}_{i-1}) d\mathbf{x}_0 \cdots d\mathbf{x}_k,$$

where  $\mathbf{Z}_{1:k}$  is the marginal likelihood of  $\mathbf{y}_{1:k}$ . The joint smoothing distribution (5) can be analytically computed through a KS, such as the RTS smoother, in the case of affine functions  $\mathbf{f}$  and  $\mathbf{h}$  [2], [32]. For completeness, the computational steps of the KS are given in Alg. 1, where  $k|K$  indicates an estimate at time  $k$  given measurements up until and including time  $K$ .

On the other hand, the filtering problem involves computing the marginal posteriors

$$p(\mathbf{x}_k|\mathbf{y}_{1:k}) = \frac{p(\mathbf{y}_k|\mathbf{x}_k) \int_{\mathcal{X}} p(\mathbf{x}_k|\mathbf{x}_{k-1}) p(\mathbf{x}_{k-1}|\mathbf{y}_{1:k-1}) d\mathbf{x}_{k-1}}{\mathbf{Z}_k} \quad (6)$$

$$\mathbf{Z}_k \triangleq \int_{\mathcal{X}} p(\mathbf{y}_k|\mathbf{x}_k) p(\mathbf{x}_k|\mathbf{x}_{k-1}) p(\mathbf{x}_{k-1}|\mathbf{y}_{1:k-1}) d\mathbf{x}_{k-1} d\mathbf{x}_k,$$

for all times  $k$ . Similarly, if  $\mathbf{f}$  and  $\mathbf{h}$  are affine, the analytical solution is given by the Kalman filter [1], which can also be found in Alg. 1. In the general case, neither the smoothing nor the marginal posteriors can be analytically computed. To address this, we next discuss linearization-based approximations.

### B. Linearization-based Estimation

Linearization-based estimation can generally be viewed as approximating the transition and measurement densities, *i.e.*,

$$p(\mathbf{x}_{k+1}|\mathbf{x}_k) \stackrel{a}{\approx} q(\mathbf{x}_{k+1}|\mathbf{x}_k), \quad p(\mathbf{y}_k|\mathbf{x}_k) \stackrel{a}{\approx} q(\mathbf{y}_k|\mathbf{x}_k),$$

where  $q(\mathbf{x}_{k+1}|\mathbf{x}_k)$  and  $q(\mathbf{y}_k|\mathbf{x}_k)$  are the respective approximations. In particular, linearization-based filters and smoothers assume affine Gaussian densities for  $q(\mathbf{x}_{k+1}|\mathbf{x}_k)$  and  $q(\mathbf{y}_k|\mathbf{x}_k)$  and the KF or KS is then applied to this approximate model. We will next detail the typical strategies employed in finding  $q(\mathbf{x}_{k+1}|\mathbf{x}_k)$  and  $q(\mathbf{y}_k|\mathbf{x}_k)$  by means of linearization.

1) *Time Update*: When computing (6), two integrals need to be evaluated. Firstly, the Chapman-Kolmogorov equation

$$p(\mathbf{x}_k|\mathbf{y}_{1:k-1}) = \int_{\mathcal{X}} p(\mathbf{x}_k|\mathbf{x}_{k-1}) p(\mathbf{x}_{k-1}|\mathbf{y}_{1:k-1}) d\mathbf{x}_{k-1}, \quad (7)$$

which, if  $p(\mathbf{x}_{k-1}|\mathbf{y}_{1:k-1})$  is Gaussian, has a closed form solution given by (10), provided that  $p(\mathbf{x}_k|\mathbf{x}_{k-1})$  is Gaussian

---

**Alg. 1** Kalman smoother
 

---

1) Time update

$$\hat{\mathbf{x}}_{k+1|k} = \mathbf{A}_f \hat{\mathbf{x}}_{k|k} + \mathbf{b}_f \quad (10a)$$

$$\mathbf{P}_{k+1|k} = \mathbf{A}_f \mathbf{P}_{k|k} \mathbf{A}_f^\top + \mathbf{Q} + \mathbf{\Omega}_f. \quad (10b)$$

2) Measurement update

$$\hat{\mathbf{x}}_{k|k} = \hat{\mathbf{x}}_{k|k-1} + \mathbf{K}_k (\mathbf{y}_k - \mathbf{A}_h \hat{\mathbf{x}}_{k|k-1} - \mathbf{b}_h) \quad (11a)$$

$$\mathbf{P}_{k|k} = \mathbf{P}_{k|k-1} - \mathbf{K}_k \mathbf{A}_h \mathbf{P}_{k|k-1} \quad (11b)$$

$$\mathbf{K}_k \triangleq \mathbf{P}_{k|k-1} \mathbf{A}_h^\top (\mathbf{A}_h \mathbf{P}_{k|k-1} \mathbf{A}_h^\top + \mathbf{R} + \mathbf{\Omega}_h)^{-1}. \quad (11c)$$

3) Smoothing step

$$\hat{\mathbf{x}}_{k|K} = \hat{\mathbf{x}}_{k|k} + \mathbf{G}_k (\hat{\mathbf{x}}_{k+1|K} - \hat{\mathbf{x}}_{k+1|k}) \quad (12a)$$

$$\mathbf{P}_{k|K} = \mathbf{P}_{k|k} + \mathbf{G}_k (\mathbf{P}_{k+1|K} - \mathbf{A}_f \mathbf{P}_{k|k} \mathbf{A}_f^\top - \mathbf{Q} - \mathbf{\Omega}_f) \mathbf{G}_k^\top \quad (12b)$$

$$\mathbf{G}_k \triangleq \mathbf{P}_{k|k} \mathbf{A}_f^\top (\mathbf{A}_f \mathbf{P}_{k|k} \mathbf{A}_f^\top + \mathbf{Q} + \mathbf{\Omega}_f)^{-1} \quad (12c)$$


---

and (2a) is affine. Given that (3a) is Gaussian, we thus seek an affine approximation of the transition function  $\mathbf{f}$  as

$$\mathbf{f}(\mathbf{x}_{k-1}) \approx \mathbf{A}_f \mathbf{x}_{k-1} + \mathbf{b}_f + \eta_f, \quad (8)$$

where  $p(\eta_f) = \mathcal{N}(\eta_f; \mathbf{0}, \mathbf{\Omega}_f)$ , capturing the error of the linearized model. Consequently, we approximate the transition density  $p(\mathbf{x}_k | \mathbf{x}_{k-1})$  as

$$q(\mathbf{x}_k | \mathbf{x}_{k-1}) = \mathcal{N}(\mathbf{x}_k; \mathbf{A}_f \mathbf{x}_{k-1} + \mathbf{b}_f, \mathbf{Q} + \mathbf{\Omega}_f). \quad (9)$$

The parameters  $\mathbf{A}_f$ ,  $\mathbf{b}_f$ , and  $\mathbf{\Omega}_f$  are typically chosen either through analytical or statistical linearization. Analytical linearization yields the EKF update, while *statistical linearization* (SL) results in the various sigma-point filters, such as the UKF with the unscented transform.

2) *Measurement Update*: After approximating the time update, the measurement update proceeds with computation of the (now approximate) marginal likelihood, *i.e.*,

$$\mathbf{Z}_k \approx \int_{\mathcal{X}} p(\mathbf{y}_k | \mathbf{x}_k) q(\mathbf{x}_k | \mathbf{y}_{1:k-1}) d\mathbf{x}_k. \quad (13)$$

Similar to (8), (13) has a closed form solution if  $p(\mathbf{y}_k | \mathbf{x}_k)$  is Gaussian and (2b) is affine. Therefore, since (3b) is Gaussian, we seek an affine approximation of the measurement function  $\mathbf{h}$  as

$$\mathbf{h}(\mathbf{x}_k) \approx \mathbf{A}_h \mathbf{x}_k + \mathbf{b}_h + \eta_h, \quad (14)$$

where  $p(\eta_h) = \mathcal{N}(\eta_h; \mathbf{0}, \mathbf{\Omega}_h)$ . Thus, the measurement density  $p(\mathbf{y}_k | \mathbf{x}_k)$  is approximated as

$$q(\mathbf{y}_k | \mathbf{x}_k) = \mathcal{N}(\mathbf{y}_k; \mathbf{A}_h \mathbf{x}_k + \mathbf{b}_h, \mathbf{R} + \mathbf{\Omega}_h). \quad (15)$$

With (9) and (15), the approximate marginal posterior (6) is now given by

$$q(\mathbf{x}_k | \mathbf{y}_{1:k}) = \frac{q(\mathbf{y}_k | \mathbf{x}_k) q(\mathbf{x}_k | \mathbf{y}_{1:k-1})}{\int_{\mathcal{X}} q(\mathbf{y}_k | \mathbf{x}_k) q(\mathbf{x}_k | \mathbf{y}_{1:k-1}) d\mathbf{x}_k}, \quad (16)$$

which is analytically tractable and given by (11). Notably, analytical linearization in (14) around the expected value of  $q(\mathbf{x}_k | \mathbf{y}_{1:k-1})$  yields the EKF measurement update, while SL recovers the different sigma-point measurement update(s).

3) *Linearization Strategies*: Given a nonlinear model

$$\mathbf{z} = \mathbf{g}(\mathbf{x}),$$

we wish to find an affine representation

$$\mathbf{g}(\mathbf{x}) \approx \mathbf{A}\mathbf{x} + \mathbf{b} + \eta, \quad (17)$$

where  $\eta \sim \mathcal{N}(\eta; \mathbf{0}, \mathbf{\Omega})$ . There are three free parameters in the affine approximation:  $\mathbf{A}$ ,  $\mathbf{b}$  and  $\mathbf{\Omega}$ . Analytical linearization, through first-order Taylor expansion, selects the parameters as

$$\mathbf{A} = \frac{d}{d\mathbf{x}} \mathbf{g}(\mathbf{x})|_{\mathbf{x}=\bar{\mathbf{x}}}, \quad \mathbf{b} = \mathbf{g}(\mathbf{x})|_{\mathbf{x}=\bar{\mathbf{x}}} - \mathbf{A}\bar{\mathbf{x}}, \quad \mathbf{\Omega} = \mathbf{0}, \quad (18)$$

where  $\bar{\mathbf{x}}$  is the point about which the function  $\mathbf{g}(\mathbf{x})$  is linearized. Note that  $\mathbf{\Omega} = \mathbf{0}$  essentially implies that the linearization is assumed to be error-free, even though there exist higher-order alternatives.

*Statistical linearization* (SL) instead linearizes w.r.t. a distribution  $p(\mathbf{x})$ , which in practice can be viewed as linear regression with samples from  $p(\mathbf{x})$  transformed through  $\mathbf{g}(\mathbf{x})$ . Assuming that such a distribution  $p(\mathbf{x}) = \mathcal{N}(\mathbf{x}; \hat{\mathbf{x}}, \mathbf{P})$  is given, SL selects the affine parameters as

$$\mathbf{A} = \Psi^\top \mathbf{P}^{-1} \quad (19a)$$

$$\mathbf{b} = \bar{\mathbf{z}} - \mathbf{A}\hat{\mathbf{x}} \quad (19b)$$

$$\mathbf{\Omega} = \Phi - \mathbf{A}\mathbf{P}\mathbf{A}^\top \quad (19c)$$

$$\bar{\mathbf{z}} = \mathbb{E}[\mathbf{g}(\mathbf{x})] \quad (19d)$$

$$\Psi = \mathbb{E}[(\mathbf{x} - \hat{\mathbf{x}})(\mathbf{g}(\mathbf{x}) - \bar{\mathbf{z}})^\top] \quad (19e)$$

$$\Phi = \mathbb{E}[(\mathbf{g}(\mathbf{x}) - \bar{\mathbf{z}})(\mathbf{g}(\mathbf{x}) - \bar{\mathbf{z}})^\top], \quad (19f)$$

where the expectations are taken w.r.t.  $p(\mathbf{x})$ . The major difference from analytical linearization is that typically  $\mathbf{\Omega} \neq \mathbf{0}$ , implying that the linearization error is captured. Typically, the expectations in (19) are not analytically tractable and practically, one often resorts to some numerical integration technique, such as the unscented transform. Note that the parameter choices in (19) can be derived by minimizing the MSE between the function  $\mathbf{g}(\mathbf{x})$  and the corresponding affine approximation. A more comprehensive discussion is out of the scope of this paper, but for additional details see, *e.g.*, [33].

### C. Discussion

The quality of the approximate marginal posterior (16) directly depends on the approximations (9) and (15). In turn, the quality of (9) and (15) directly depend on the linearization points (densities), typically chosen as the previous approximate posterior and approximate predictive distributions. To improve the approximation of the measurement density (15), iterated filters, such as the IEKF, IUKF or IPLF have been proposed [20]–[22], [24].

However, except for [34], none of these algorithms address the approximate transition density (9), despite its direct impact on the approximate marginal posterior. Typically, this is motivated by the fact that nonlinearities in the measurement model affect the resulting posterior approximation to a greater extent than the transition model. Nevertheless, by accounting for the linearization error in the transition model  $\mathbf{f}$ , the performance of iterated filters can be improved even further. Furthermore,

standard iterated filters are not even useful in the case of a nonlinear transition function  $\mathbf{f}$  but linear measurement function  $\mathbf{h}$ , even though the linearization of  $\mathbf{f}$  also affects the quality of the approximate posterior. To address this limitation, we propose a linearization-based family of methods that encompasses both the transition density as well as the measurement density approximations.

### III. DYNAMICALLY ITERATED FILTERS

We here recapitulate the main points of our derivation in [31], where we first derived the DIFs. To that end, note that to optimally approximate both the transition density (9), as well as the measurement density (15) at time  $k$ , we naturally need to seek an approximate posterior over both  $\mathbf{x}_{k-1}$  and  $\mathbf{x}_k$ .

#### A. Optimal Affine Approximations

Let two auxiliary variables  $\mathbf{g}_k$  and  $\mathbf{g}_{k-1}$  be defined as

$$\mathbf{g}_{k-1} = \mathbf{f}(\mathbf{x}_{k-1}) + \psi, \quad p(\psi) = \mathcal{N}(\mathbf{0}, \alpha \mathbf{I}) \quad (20a)$$

$$\mathbf{g}_k = \mathbf{h}(\mathbf{x}_k) + \phi, \quad p(\phi) = \mathcal{N}(\mathbf{0}, \beta \mathbf{I}) \quad (20b)$$

where  $\psi$  and  $\phi$  are independent of each other as well as the process noise  $\mathbf{w}_k$  and the measurement noise  $\mathbf{e}_k$ . Note that  $\mathbf{g}_{k-1} \rightarrow \mathbf{f}(\mathbf{x}_{k-1})$  and  $\mathbf{g}_k \rightarrow \mathbf{h}(\mathbf{x}_k)$  as  $\alpha, \beta \rightarrow 0$ . The true joint posterior of  $\mathbf{x}_{k-1}$ ,  $\mathbf{x}_k$ ,  $\mathbf{g}_{k-1}$  and  $\mathbf{g}_k$  is then given by

$$\begin{aligned} & p(\mathbf{x}_{k-1:k}, \mathbf{g}_{k-1:k} | \mathbf{y}_{1:k}) \\ & \propto p(\mathbf{x}_{k-1:k} | \mathbf{y}_{1:k}) p(\mathbf{g}_k | \mathbf{x}_k) p(\mathbf{g}_{k-1} | \mathbf{x}_{k-1}). \end{aligned} \quad (21)$$

We assume that the approximate posterior decomposes in a similar manner, *i.e.*,

$$\begin{aligned} & q_\theta(\mathbf{x}_{k-1:k}, \mathbf{g}_{k-1:k} | \mathbf{y}_{1:k}) \\ & \approx q_\theta(\mathbf{x}_{k-1:k} | \mathbf{y}_{1:k}) q_\theta(\mathbf{g}_k | \mathbf{x}_k) q_\theta(\mathbf{g}_{k-1} | \mathbf{x}_{k-1}). \end{aligned} \quad (22)$$

Here,  $\theta$  are the parameters of the affine approximation of the transition model and measurement model, *i.e.*,  $\theta = [\mathbf{A}_f, \mathbf{b}_f, \mathbf{\Omega}_f, \mathbf{A}_h, \mathbf{b}_h, \mathbf{\Omega}_h]$ .

The parameters  $\theta$  should then be chosen such that  $q_\theta(\mathbf{x}_{k-1:k}, \mathbf{g}_{k-1:k} | \mathbf{y}_{1:k})$  closely approximates  $p(\mathbf{x}_{k-1:k}, \mathbf{g}_{k-1:k} | \mathbf{y}_{1:k})$ . Specifically, the optimal parameters  $\theta^*$ , and thus the optimal affine approximations of  $\mathbf{f}$  and  $\mathbf{h}$ , are found by minimizing a loss  $\mathcal{L}(\theta)$ , *i.e.*,

$$\theta^* = \arg \min_{\theta} \mathcal{L}(\theta). \quad (23)$$

The loss  $\mathcal{L}(\theta)$  is chosen as the *Kullback–Leibler* (KL) divergence between the true and approximate posterior, *i.e.*

$$\begin{aligned} \mathcal{L}(\theta) & \triangleq \text{KL}(p(\mathbf{x}_{k-1:k}, \mathbf{g}_{k-1:k} | \mathbf{y}_{1:k}) || q_\theta(\mathbf{x}_{k-1:k}, \mathbf{g}_{k-1:k} | \mathbf{y}_{1:k})) \\ & = \text{KL}(p(\mathbf{x}_{k-1:k} | \mathbf{y}_{1:k}) || q_\theta(\mathbf{x}_{k-1:k} | \mathbf{y}_{1:k})) \\ & \quad + \mathbb{E}[\text{KL}(p(\mathbf{g}_k | \mathbf{x}_k) || q_\theta(\mathbf{g}_k | \mathbf{x}_k))] \\ & \quad + \mathbb{E}[\text{KL}(p(\mathbf{g}_{k-1} | \mathbf{x}_{k-1}) || q_\theta(\mathbf{g}_{k-1} | \mathbf{x}_{k-1}))], \end{aligned} \quad (24)$$

where the expectations in  $\mathcal{L}(\theta)$  are taken w.r.t. the true joint posterior  $p(\mathbf{x}_{k-1:k}, \mathbf{y}_{1:k})$ . See [31] for the derivation of (24). Note that  $\mathcal{L}(\theta)$  can be decomposed into three distinct terms, each dealing with a specific factor of (22). The first term ensures that the true and approximate joint posterior of the

state at time  $k$  and  $k-1$  are close. The remaining two terms minimize the discrepancy between the affine approximations and the true measurement and transition model, respectively.

Since the expectations in  $\mathcal{L}(\theta)$  are taken w.r.t. the true joint posterior  $p(\mathbf{x}_{k-1:k} | \mathbf{y}_{1:k})$ , minimizing the loss (24) is, unfortunately, impractical. Nevertheless, an iterative approach can be used to approximately solve this minimization problem.

#### B. Iterative Solution

In order to practically optimize (23), we assume access to an  $i^{\text{th}}$  approximation to the state joint posterior  $p(\mathbf{x}_{k-1:k} | \mathbf{y}_{1:k}) \approx q_\theta^i(\mathbf{x}_{k-1:k} | \mathbf{y}_{1:k})$ . Subsequently, we substitute  $q_\theta^i(\mathbf{x}_{k-1:k} | \mathbf{y}_{1:k})$  for  $p(\mathbf{x}_{k-1:k} | \mathbf{y}_{1:k})$  in (24) and thus optimize an approximate loss, given by

$$\begin{aligned} \mathcal{L}(\theta) & \approx \mathcal{L}(\theta^i) = \text{KL}(q_\theta^i(\mathbf{x}_{k-1:k} | \mathbf{y}_{1:k}) || q_\theta^{i+1}(\mathbf{x}_{k-1:k} | \mathbf{y}_{1:k})) \\ & \quad + \mathbb{E}_{q_\theta^i(\mathbf{x}_{k-1:k} | \mathbf{y}_{1:k})} [\text{KL}(p(\mathbf{g}_k | \mathbf{x}_k) || q_\theta^{i+1}(\mathbf{g}_k | \mathbf{x}_k))] \\ & \quad + \mathbb{E}_{q_\theta^i(\mathbf{x}_{k-1:k} | \mathbf{y}_{1:k})} [\text{KL}(p(\mathbf{g}_{k-1} | \mathbf{x}_{k-1}) || q_\theta^{i+1}(\mathbf{g}_{k-1} | \mathbf{x}_{k-1}))], \end{aligned}$$

where the expectations are now over  $q_\theta^i(\mathbf{x}_{k-1:k} | \mathbf{y}_{1:k})$ . Sufficiently close to a fixed point, the first KL term is approximately 0, simplifying the approximate loss to

$$\begin{aligned} \mathcal{L}(\theta^i) & \approx \mathbb{E}_{q_\theta^i(\mathbf{x}_{k-1:k} | \mathbf{y}_{1:k})} \left[ \text{KL}(p(\mathbf{g}_k | \mathbf{x}_k) || q_\theta^{i+1}(\mathbf{g}_k | \mathbf{x}_k)) \right. \\ & \quad \left. + \text{KL}(p(\mathbf{g}_{k-1} | \mathbf{x}_{k-1}) || q_\theta^{i+1}(\mathbf{g}_{k-1} | \mathbf{x}_{k-1})) \right]. \end{aligned} \quad (25)$$

Technically, the optimal  $\theta^*$  is given by SL of  $\mathbf{f}$  and  $\mathbf{h}$  w.r.t. the current approximation  $q_\theta^i(\mathbf{x}_{k-1:k} | \mathbf{y}_{1:k})$ , see *e.g.*, [23]. This only requires the marginal  $q_\theta^i(\mathbf{x}_{k-1} | \mathbf{y}_{1:k})$  for SL of  $\mathbf{f}$ , and similarly, the marginal  $q_\theta^i(\mathbf{x}_k | \mathbf{y}_{1:k})$  for SL of  $\mathbf{h}$ . Thus, conceptually, the solution amounts to iterating a prediction, update, and smoothing step in order to provide new linearization points (densities) for both the transition density as well as the measurement density simultaneously. These steps are repeated until fixed-point convergence, ultimately yielding an approximate posterior  $q(\mathbf{x}_{k-1:k} | \mathbf{y}_{1:k})$ . The overall algorithm is schematically depicted in Fig. 1 and is given in Alg. 2.

#### C. Illustration

We visually illustrate the DIFs by applying the analytically linearized DIF, the *dynamically iterated extended Kalman filter* (DIEKF), to a one-dimensional model given by

$$\mathbf{x}_{k+1} \sim \mathcal{N}(\mathbf{x}_{k+1}; a\mathbf{x}_k^3, Q)$$

$$\mathbf{y}_k \sim \mathcal{N}(\mathbf{y}_k; \mathbf{x}_k, R)$$

$$p(\mathbf{x}_{k-1} | \mathbf{y}_{1:k-1}) = \mathcal{N}(\mathbf{x}_{k-1}; 3, 4),$$

where  $a = 0.01, Q = 0.1$  and  $R = 0.1$ . The approximate densities produced by the DIEKF are visualized in Fig. 2, where two iterations are enough to yield a good posterior approximation. The true posterior is found simply by evaluating the posterior density over a dense grid.

#### D. Discussion

Unlike regular iterated filters, the DIF proves valuable across all potential combinations of models with linear and nonlinear

---

**Alg. 2** Dynamically iterated filter
 

---

**Require:**  $q(\mathbf{x}_{k-1}|y_{1:k-1}) = \mathcal{N}(\mathbf{x}_{k-1}; \hat{\mathbf{x}}_{k-1|k-1}, \mathbf{P}_{k-1|k-1})$

- 1: Linearize  $\mathbf{f}$  about  $\hat{\mathbf{x}}_{k-1|k-1}, \mathbf{P}_{k-1|k-1}$  by (18) or (19)
  - 2: Compute  $\hat{\mathbf{x}}_{k|k-1}^0, \mathbf{P}_{k|k-1}^0$  by (10)
  - 3: Linearize  $\mathbf{h}$  about  $\hat{\mathbf{x}}_{k|k-1}^0, \mathbf{P}_{k|k-1}^0$  by (18) or (19)
  - 4: Compute  $\hat{\mathbf{x}}_{k|k}^0, \mathbf{P}_{k|k}^0$  by (11)
  - 5: Compute  $\hat{\mathbf{x}}_{k-1|k}^0, \mathbf{P}_{k-1|k}^0$  by (12)
  - 6:  $\hat{\mathbf{x}}_{k-1|k}, \mathbf{P}_{k-1|k}, \hat{\mathbf{x}}_{k|k}, \mathbf{P}_{k|k} \leftarrow$  Alg. 3 or Alg. 5
  - 7: **return**  $\hat{\mathbf{x}}_{k|k}, \mathbf{P}_{k|k}$  (and  $\hat{\mathbf{x}}_{k-1|k}, \mathbf{P}_{k-1|k}$ )
- 

**Alg. 3** Inner loop of DIF
 

---

**Require:**  $\hat{\mathbf{x}}_{k-1|k-1}, \mathbf{P}_{k-1|k-1}, \hat{\mathbf{x}}_{k-1|k}^0, \mathbf{P}_{k-1|k}^0, \hat{\mathbf{x}}_{k|k}^0, \mathbf{P}_{k|k}^0$

- 1:  $i \leftarrow 0$
  - 2: **while** not converged **do**
  - 3:  $\bar{\mathbf{x}}_{k-1}, \bar{\mathbf{P}}_{k-1}, \bar{\mathbf{x}}_k, \bar{\mathbf{P}}_k \leftarrow \hat{\mathbf{x}}_{k-1|k}^i, \mathbf{P}_{k-1|k}^i, \hat{\mathbf{x}}_{k|k}^i, \mathbf{P}_{k|k}^i$
  - 4:  $\hat{\mathbf{x}}_{k-1|k}^{i+1}, \mathbf{P}_{k-1|k}^{i+1}, \hat{\mathbf{x}}_{k|k}^{i+1}, \mathbf{P}_{k|k}^{i+1} \leftarrow$  Alg. 4
  - 5:  $i \leftarrow i + 1$
  - 6: **end while**
- 

**Alg. 4** Single step of a DIF
 

---

**Require:**  $\hat{\mathbf{x}}_{k-1|k-1}, \mathbf{P}_{k-1|k-1}, \bar{\mathbf{x}}_{k-1}, \bar{\mathbf{P}}_{k-1}, \bar{\mathbf{x}}_k, \bar{\mathbf{P}}_k$

- 1: Linearize  $\mathbf{f}$  about  $\bar{\mathbf{x}}_{k-1}, \bar{\mathbf{P}}_{k-1}$  by (18) or (19)
  - 2: Compute  $\hat{\mathbf{x}}_{k|k-1}, \mathbf{P}_{k|k-1}$  by (10)
  - 3: Linearize  $\mathbf{h}$  about  $\bar{\mathbf{x}}_k, \bar{\mathbf{P}}_k$  by (18) or (19)
  - 4: Compute  $\hat{\mathbf{x}}_{k|k}, \mathbf{P}_{k|k}$  by (11)
  - 5: Compute  $\hat{\mathbf{x}}_{k-1|k}, \mathbf{P}_{k-1|k}$  by (12)
  - 6: **return**  $\hat{\mathbf{x}}_{k-1|k}, \mathbf{P}_{k-1|k}, \hat{\mathbf{x}}_{k|k}, \mathbf{P}_{k|k}$
- 

functions,  $\mathbf{f}$  and  $\mathbf{h}$ . It is worth noting that the DIF functions more or less like an IPLF, but also encompasses the transition density. However, an “extended” version, *i.e.*, the DIEKF, is recovered by opting for analytical, rather than statistical, linearization. Further, similar to the IUKF in [20], an unscented version is recovered by maintaining fixed covariance matrices  $\mathbf{P}_{k-1|k}^i = \mathbf{P}_{k-1|k-1}$  and  $\mathbf{P}_{k|k}^i = \mathbf{P}_{k|k-1}$  and updating these only during the last iteration of Alg. 3. Moreover, the DIFs may also be interpreted as “local” iterated smoothers, analogous to the *iterated extended Kalman smoother* (IEKS) [35] and the *iterated posterior linearization smoother* (IPLS) [36], operating on just one time-instance and measurement. Thus, the method can be viewed as an iterated one-step fixed-lag smoother as well, a connection which we shall now firmly establish.

## IV. DAMPED DYNAMICALLY ITERATED FILTERS

For more complex, highly nonlinear, models, the DIFs may sometimes diverge, similar to standard iterated filters, such as the IEKF and IUKF. To lessen these issues, damped versions of iterated filters have been developed, where an explicit step-size has been introduced into the iterate updates, improving the (local) convergence properties [19], [20], [27]. Inspired by the successes in the development of damped iterated filters, we shall now apply a similar reasoning to develop damped DIFs, to reap similar benefits in terms of convergence properties.

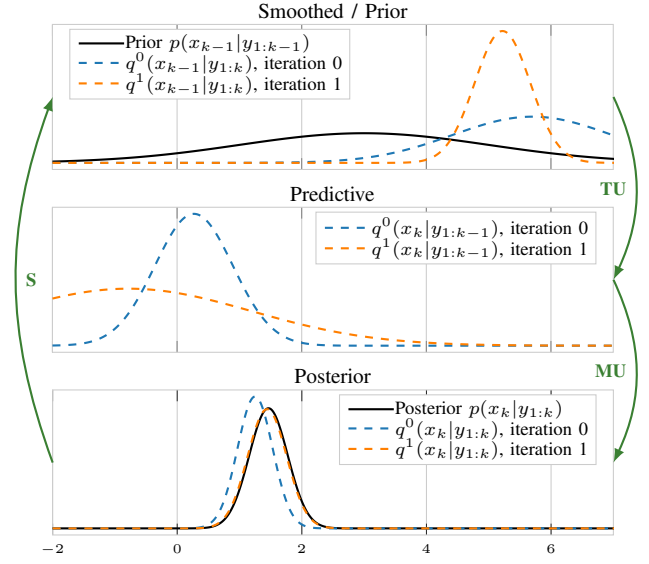


Fig. 2: Illustration of the (extended) DIF. The filter moves from the prior (top) to the predictive (middle), via the time update (TU), to the posterior (bottom), via the measurement update (MU), and back up to the smoothed (top), via the smoothing step (S). Notice that iteration 0 exactly corresponds to an EKF.

To that end, we first establish a connection between DIFs and iterated approximate RTS smoothers. This will allow us to interpret the DIFs as GN methods, which in turn lets us introduce explicit step-sizes in the iterate updates, thereby improving local convergence properties of the DIFs.

## A. DIF as a GN Algorithm

The loss function (24) is suitable to motivate the iterative procedure of the DIFs. However, as the expected KL-terms in (24) are not analytically tractable, it is not wise to use (24) to select a step-size. Thus, we require another criteria for step-size selection and establish the following proposition.

**Proposition 1** (Loss function). *In each time step  $k$ , DIFs minimize*

$$2\mathcal{L}(\mathbf{x}_{k-1}, \mathbf{x}_k) = \|\mathbf{x}_{k-1} - \mathbf{x}_{k-1|k-1}\|_{\mathbf{P}_{k-1|k-1}}^2 + \|\mathbf{y}_k - \mathbf{h}(\mathbf{x}_k)\|_{\mathbf{R} + \Omega_{\mathbf{h}}}^2 + \|\mathbf{x}_k - \mathbf{f}(\mathbf{x}_{k-1})\|_{\mathbf{Q} + \Omega_{\mathbf{f}}}^2, \quad (26)$$

where  $\|\mathbf{v}\|_{\mathbf{S}}^2 = \mathbf{v}^\top \mathbf{S}^{-1} \mathbf{v}$ .

*Proof:* See Appendix A. ■

Proposition 1 establishes the loss function that DIFs minimize, a dynamical analog to the loss functions of the IEKF, IUKF and IPLF. There is, however, a caveat. Notice that (26) depends on  $\Omega_{\mathbf{f}}, \Omega_{\mathbf{h}}$ , *i.e.*, the linearization error of  $\mathbf{f}$  and  $\mathbf{h}$ . In the analytically linearized DIEKF, this is not an issue as the linearization error is not explicitly dealt with. However, in the *dynamically iterated unscented Kalman filter* (DIUKF) and *dynamically iterated posterior linearization filter* (DIPLF), the linearization errors are recomputed in each iteration, meaning that the weighting of the loss changes

$$2\mathcal{L}^i(\mathbf{x}_{k-1}, \mathbf{x}_k) = \|\mathbf{x}_{k-1} - \mathbf{x}_{k-1|k-1}\|_{\mathbf{P}_{k-1|k-1}}^2 + \|\mathbf{y}_k - \mathbf{h}(\mathbf{x}_k)\|_{\mathbf{R} + \Omega_{\mathbf{h}}^i}^2 + \|\mathbf{x}_k - \mathbf{f}(\mathbf{x}_{k-1})\|_{\mathbf{Q} + \Omega_{\mathbf{f}}^i}^2, \quad (27)$$

---

**Alg. 5** Inner loop of the damped DIUKF/DIEKF
 

---

**Require:**  $\hat{\mathbf{x}}_{k-1|k-1}, \mathbf{P}_{k-1|k-1}, \hat{\mathbf{x}}_{k-1|k}^0, \mathbf{P}_{k-1|k}^0, \hat{\mathbf{x}}_{k|k}^i, \mathbf{P}_{k|k}^0$   
 $i \leftarrow 0$   
**while** not converged **do**  
 $\bar{\mathbf{x}}_{k-1}, \bar{\mathbf{P}}_{k-1}, \bar{\mathbf{x}}_k, \bar{\mathbf{P}}_k \leftarrow \hat{\mathbf{x}}_{k-1|k}^i, \mathbf{P}_{k-1|k}^0, \hat{\mathbf{x}}_{k|k}^i, \mathbf{P}_{k|k}^0$   
 $\xi_{k-1}, -, \xi_k, - \leftarrow$  Alg. 4  $\triangleright$  Propose new iterates  
 $\mathbf{x}^i = \begin{bmatrix} \hat{\mathbf{x}}_{k-1|k}^i \\ \hat{\mathbf{x}}_{k|k}^i \end{bmatrix}, \mathbf{p}^i = \begin{bmatrix} \xi_{k-1} - \hat{\mathbf{x}}_{k-1|k}^i \\ \xi_k - \hat{\mathbf{x}}_{k|k}^i \end{bmatrix}, \alpha \leftarrow 1$   
**while**  $\mathcal{L}(\mathbf{x}^i + \alpha \mathbf{p}^i) \leq \mathcal{L}(\mathbf{x}^i)$  **do**  
 $\alpha \leftarrow \alpha/\eta$   $\triangleright$  Other strategies possible  
**end while**  
Set  $\begin{bmatrix} \hat{\mathbf{x}}_{k-1|k}^{i+1} \\ \hat{\mathbf{x}}_{k|k}^{i+1} \end{bmatrix} \leftarrow \mathbf{x}^i + \alpha \mathbf{p}^i$   
 $i \leftarrow i + 1$   
**end while**  
 $\bar{\mathbf{x}}_{k-1}, \bar{\mathbf{P}}_{k-1}, \bar{\mathbf{x}}_k, \bar{\mathbf{P}}_k \leftarrow \hat{\mathbf{x}}_{k-1|k}^i, \mathbf{P}_{k-1|k}^0, \hat{\mathbf{x}}_{k|k}^i, \mathbf{P}_{k|k}^0$   
 $-, \mathbf{P}_{k-1|k}^i, -, \mathbf{P}_{k|k}^i \leftarrow$  Alg. 4  $\triangleright$  Covariance update  
**return**  $\bar{\mathbf{x}}_{k-1}, \bar{\mathbf{P}}_{k-1}, \bar{\mathbf{x}}_k, \bar{\mathbf{P}}_k$

---

which does not necessarily yield a monotonic cost decrease for decreasing residuals (note the dependence of  $\Omega$  on  $i$ ). For the DIUKF, this is not a problem, as the state covariance is already “frozen” until the last iterate update. For the DIPLF on the other hand, we propose to remedy this problem by constructing an inner and outer loop, similar but not identical to that of [27]. The inner loop is identical to that of the DIUKF, where only the estimated mean is updated. The outer loop on the other hand updates the state covariance and re-runs the inner loop. This is then repeated until some convergence criteria is fulfilled, *e.g.*, the KL divergence between two successive approximations is negligible. Hence, the damped DIPLF is essentially an iterated damped DIUKF, *i.e.*, a “doubly” iterated DIUKF. The general damped DIF is given in Alg. 2, with the choice of Alg. 5 on Line 6. In particular, Alg. 5 is the version *without* the outer loop. The only difference is that Alg. 5 is rerun several times, with new covariances  $\mathbf{P}_{k-1|k}^0$  and  $\mathbf{P}_{k|k}^0$  each time, given by the last iteration.

### B. Step-size correction

Through Proposition 1, we can establish that the DIFs are closely related to approximate one-step fixed-lag RTS smoothers. As such, we can interpret the DIFs as GN methods and can therefore introduce step-size correction to improve local convergence properties.

To that end, let the GN iterate be defined by  $\mathbf{x}^i = [\mathbf{x}_{k-1}^{i,\top}, \mathbf{x}_k^{i,\top}]^\top$ . A step-size,  $\alpha^i$ , can then be introduced to the iterate update as

$$\mathbf{x}^{i+1} = \mathbf{x}^i + \alpha^i \mathbf{p}^i,$$

with the step  $\mathbf{p}^i$ . The step is given by

$$\mathbf{p}^i = -(\mathbf{J}^{i,\top} \mathbf{J}^i)^{-1} \mathbf{J}^{i,\top} \mathbf{r}^i, \quad (28)$$

where

$$\mathbf{J}^i = \left. \frac{d\mathbf{r}^i(\mathbf{s})}{d\mathbf{s}} \right|_{\mathbf{s}=\mathbf{x}^i}. \quad (29)$$

Here,

$$\mathbf{r}(\mathbf{x}^i) = \begin{bmatrix} \mathbf{P}_{k-1|k-1}^{-1/2} (\mathbf{x}_{k-1} - \mathbf{x}_{k-1|k-1}) \\ (\mathbf{R} + \Omega_{\mathbf{h}}^*)^{-1/2} (\mathbf{y}_k - \mathbf{h}(\mathbf{x}_k)) \\ (\mathbf{Q} + \Omega_{\mathbf{f}}^*)^{-1/2} (\mathbf{x}_k - \mathbf{f}(\mathbf{x}_{k-1})) \end{bmatrix}, \quad (30)$$

where  $\star$  corresponds to the two different  $\Omega_{\mathbf{h}}$  and  $\Omega_{\mathbf{f}}$  in (26), and (27), respectively. The step  $\mathbf{p}^i$  can equivalently be defined as

$$\mathbf{p}^i = \xi^{i+1} - \mathbf{x}^i,$$

which we use in Alg. 5. Here, the expression for  $\xi^{i+1}$  is given immediately by a single step of the DIF, *i.e.*, Alg. 4. This can be seen as proposing a new iterate  $\xi^{i+1}$  through the KS in Alg. 1 and weighing its influence by  $\alpha^i$ .

Due to, *e.g.*, noise, poor Hessian approximation, or strong non-linearities, a full step  $\alpha^i = 1$ , *i.e.*, choosing  $\xi^{i+1}$  as the new iterate, may not yield a cost decrease, *i.e.*,

$$\mathcal{L}^*(\mathbf{x}^i + \alpha^i \mathbf{p}^i) \not\leq \mathcal{L}^*(\mathbf{x}^i).$$

Given the cost functions and control over the step-size one can find an  $\alpha^i \in (0, 1]$  such that

$$\mathcal{L}^*(\mathbf{x}^i + \alpha^i \mathbf{p}^i) \leq \mathcal{L}^*(\mathbf{x}^i),$$

which is called a line-search. For more elaborate line-search strategies, we refer to, *e.g.*, [28].

### C. Discussion

Our construction for the DIPLF is heavily inspired by [27]. There is, however, a distinct difference in our construction of the inner loop. Particularly, [27] freeze  $\Omega$  in their inner loop construction, in order to guarantee a monotonic cost decrease within the inner loop. In contrast, we argue that this is not conceptually sound and can in fact hinder convergence. Within the inner loop, the model is still re-linearized in each step and the linearization error  $\Omega$  is used in the iterate update. Therefore, freezing it does not take the new linearization point (distribution) into account. Further, a connection was recently established between iterated statistical linearization and quasi-Newton [37]. In particular, in [37] it was shown that the IPLF, IUKF and *iterated cubature Kalman filter* (ICKF) are in fact quasi-Newton methods with very particular choices of Hessian correction. Therefore, excluding the linearization error  $\Omega$  from the inner loop may actually lead to suboptimal step lengths. However, we should point out that from our practical experience, this change to the inner loop seems to make little difference in practice. There may exist problems where this does make a difference, but we are yet to find one. Our changes to the inner loop are thus purely for conceptual reasons and we shall not investigate it further in this paper.

## V. NUMERICAL EXAMPLES

Next, we present three numerical examples illustrating the application of DIFs and their damped counterparts. The first example consists of an artificial highly nonlinear one-dimensional problem that motivates the usage of damping in the DIFs. The second example is a simulated maneuvering target tracking problem where the dynamics are nonlinear

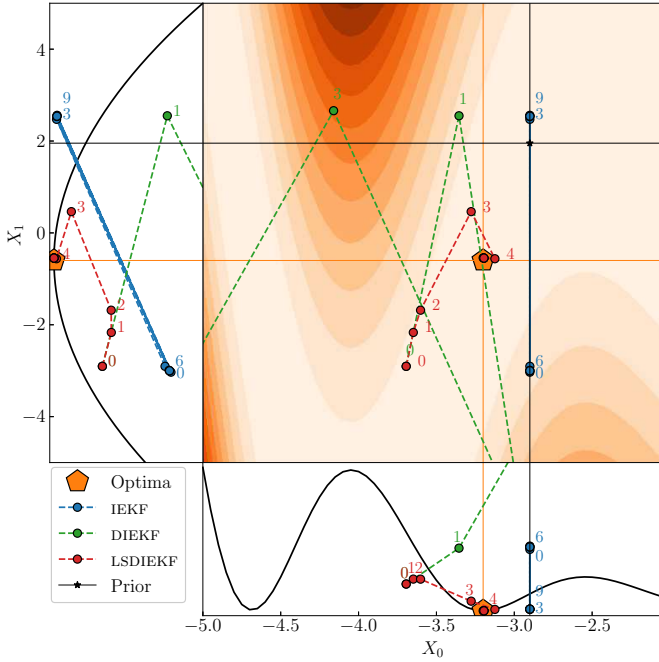


Fig. 3: The loss landscape of the first example as well as the iterates produced by the IEKF, DIEKF and LSDIEKF. The contour plot illustrates the 2D loss landscape over the states  $X_0$  and  $X_1$ , where a lighter orange corresponds to a lower loss. Further, the two one-dimensional subplots illustrate the marginal loss curves at the optimal  $X_0$  and  $X_1$ , respectively.

but the measurement model is *linear*. The third example is an acoustic localization problem where both dynamics and measurements are nonlinear. Note that, in the first and third examples, we focus solely on the “extended” variants of the DIFs to keep the numerical results uncluttered. In the second example, we consider the DIEKF, DIUKF, and DIPLF, but not their respective damped versions, again to reduce clutter.

### A. One-Dimensional Nonlinear

In this example, we consider an artificial system given by

$$\mathbf{x}_{k+1} = \cos(\mathbf{x}_k) \sin(\mathbf{x}_k) \mathbf{x}_k^2 + \mathbf{w}_k \quad (31a)$$

$$\mathbf{y}_k = \arctan(\mathbf{x}_k) + \mathbf{e}_k, \quad (31b)$$

with  $\mathbf{w}_k \sim \mathcal{N}(0, 0.1)$  and  $\mathbf{e}_k \sim \mathcal{N}(0, 1)$ . The true state and the prior at time 0 are given by  $x = -3.2$  and  $x_{0|0} \sim \mathcal{N}(-2.9, 1)$ , respectively. We run the IEKF, DIEKF and a *line-search dynamically iterated extended Kalman filter* (LSDIEKF) for 10 iterations each. We visualize the 2D loss landscape in Fig. 3 over the state at time 0,  $X_0$ , and time 1,  $X_1$ , and overlay the iterates produced by the IEKF, DIEKF and LSDIEKF, respectively. The two one-dimensional subplots illustrate the marginal loss curves at the optima, *i.e.*, the bottom subplot corresponds to the loss over  $X_0$  at  $X_1 = X_1^*$  where  $X_1^*$  is the optima at time 1. The black star and lines correspond to the prior means and the orange star and lines correspond to the optima. From Fig. 3, it is clear that the DIEKF (green), diverges completely. Further, the ordinary IEKF (blue), ends up in a sort of “limit cycle” behaviour, jumping between two modes. On the other hand, the LSDIEKF (red), converges to the optima.

### B. Maneuvering Target Tracking

For completeness, we here consider the same numerical example as in [31], and therefore recapitulate only the most essential information of the example. We refer to [31] for detailed information.

We consider a target maneuvering in a plane and describe the target state using the state vector  $\mathbf{x}_k = [p_k^x \ v_k^x \ p_k^y \ v_k^y \ \omega_k]^\top$ . Here,  $p_k^x$ ,  $p_k^y$ ,  $v_k^x$ , and  $v_k^y$  are the Cartesian coordinates and velocities of the target, respectively. Further,  $\omega_k$  is the turn rate. The transition model is given by

$$\mathbf{x}_{k+1} = \mathbf{f}(\mathbf{x}_k) + \mathbf{w}_k, \quad (32)$$

where

$$\mathbf{f}(\mathbf{x}_k) = \begin{bmatrix} 1 & \frac{\sin(T\omega_k)}{\omega_k} & 0 & -\frac{(1-\cos(T\omega_k))}{\omega_k} & 0 \\ 0 & \cos(T\omega_k) & 0 & -\sin(T\omega_k) & 0 \\ 0 & \frac{(1-\cos(T\omega_k))}{\omega_k} & 1 & \frac{\sin(T\omega_k)}{\omega_k} & 0 \\ 0 & \sin(T\omega_k) & 0 & \cos(T\omega_k) & 0 \\ 0 & 0 & 0 & 0 & 1 \end{bmatrix} \mathbf{x}_k,$$

and  $T$  is the sampling period. Further,  $\mathbf{w}_k \sim \mathcal{N}(\mathbf{w}_k; \mathbf{0}, \mathbf{Q})$  is the process noise at time  $k$ , with

$$\mathbf{Q} = \text{blkdiag} \left( \begin{bmatrix} q_1 \frac{T^3}{3} & q_1 \frac{T^2}{2} \\ q_1 \frac{T^2}{2} & q_1 T \end{bmatrix}, \begin{bmatrix} q_1 \frac{T^3}{3} & q_1 \frac{T^2}{2} \\ q_1 \frac{T^2}{2} & q_1 T \end{bmatrix}, q_2 \right),$$

where  $q_1$  and  $q_2$  are tunable parameters of the model. We assume a linear measurement model of the Cartesian position of the target with additive Gaussian noise given by  $\mathbf{e}_k \sim \mathcal{N}(\mathbf{e}_k; \mathbf{0}, \sigma^2 \mathbf{I})$ .

We consider 25 different noise configurations, by fixing  $q_2 = 10^{-2}$  and varying  $q_1$  and  $\sigma^2$ . We then evaluate the average RMSE, separately for position and velocity, over 200 simulations for each of the filters and their corresponding baselines. The results are presented as  $5 \times 5$  matrices, where each cell corresponds to a particular noise configuration for a particular pair of algorithms, *e.g.*, the results for the DIEKF and EKF are summarized in one matrix. The position and velocity RMSEs are presented in Fig. 5(a) and Fig. 5(b), respectively.

All of the DIFs improve upon their baselines, but the analytically linearized DIEKF improves the most, see Fig. 5(a). Surprisingly, the EKF diverges in 22/25 configurations whereas the DIEKF lowers that to 5/25, only diverging in the high noise scenario ( $\sigma^2 = 10^2$ ). The DIUKF and DIPLF improve the most in low process noise regimes, with otherwise relatively modest improvements. However, all of the DIFs substantially improve in velocity RMSE, see Fig. 5(b). For low process noise regimes the improvement is up to 10-fold for the DIEKF and 5-fold for the DIUKF and DIPLF. Even for modest noise levels, the DIUKF and DIPLF roughly manage a 2-fold performance improvement. For the high noise scenario ( $\sigma^2 = 10^2$ ), the DIUKF and DIPLF show a 10-fold performance improvement and bring the velocity RMSE down to reasonable levels where the RMSE for the UKF is very high. It is important to note that even though the measurement model is *linear*, we still see significant performance improvements as well as robustness improvements for the DIEKF in particular.

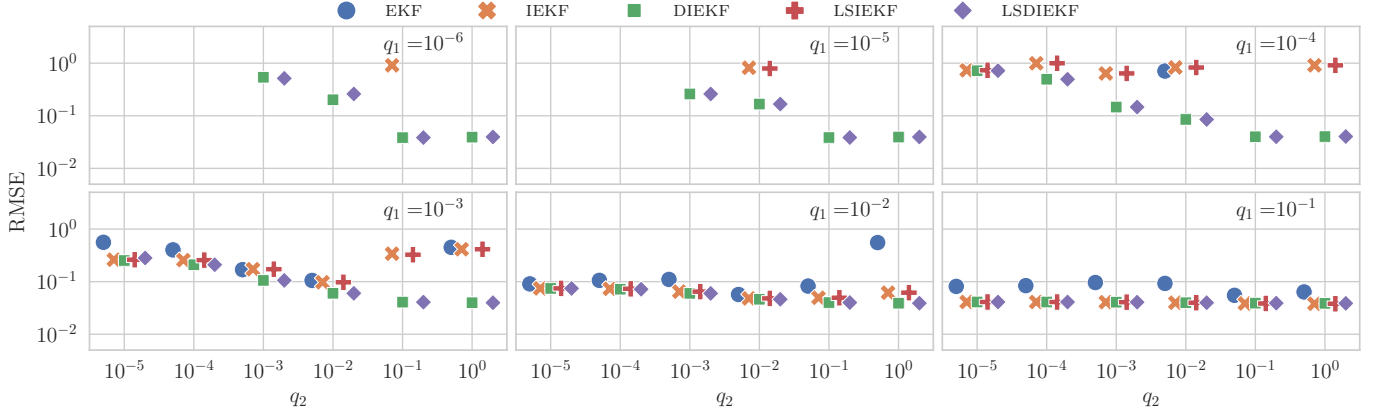


Fig. 4: Position *root mean square error* (RMSE) for the different methods and noise settings. Each subplot corresponds to a different value of  $q_1$ , indicated by the text in each subplot. An RMSE higher than approximately 1 m corresponds to a “divergent” filter based on visual inspection of resulting estimate trajectories and is left out of the plots. Note that the markers are slightly spread out to aid visibility.

### C. Acoustic Localization

We consider an acoustic localization problem where the system has both nonlinear dynamics as well as a nonlinear measurement model. In order to not clutter the results, we only consider the EKF, IEKF, DIEKF as well as the damped IEKF and DIEKF.

An RC-car is driving along a pre-defined trajectory in an enclosed area, with dynamics modeled by (32). Whilst driving, the car emits a known sound pulse at equidistant points in time. Four microphones are used to construct *time difference of arrival* (TDOA) measurements. Each measurement at microphone  $j$  is thus modeled as

$$\mathbf{y}_k^j = r_k^1 - r_k^j + \mathbf{e}_k^j, \quad j = 1, \dots, 3 \quad (33)$$

where  $r_k^j \triangleq \|[p_k^x \ p_k^y]^\top - s^j\|$ , and  $s^j$  is the 2D position of each microphone, which is assumed known. Note that (33) is parameterized in distance and not in time.

Before data collection, a calibration experiment was conducted to construct an error model for each microphone, and thus,  $\mathbf{e}_k = [\mathbf{e}_k^1 \ \mathbf{e}_k^2 \ \mathbf{e}_k^3]^\top \sim \mathcal{N}(\mathbf{0}, \mathbf{R})$  where

$$\mathbf{R} = \sigma_1^2 \mathbf{1}\mathbf{1}^\top + \text{diag}(\sigma_2^2 \ \sigma_3^2 \ \sigma_4^2),$$

where  $\sigma_j^2$  is the variance of microphone  $j$ .

We set  $q_1 = 10^{-j}$ ,  $q_2 = 10^{-l}$  and let  $j = -6, \dots, 0$ ,  $l = -5, \dots, 0$ , and sweep over all such pairs, *i.e.*, 42 different process noise configurations. For each configuration, we compute the RMSE against a ground truth trajectory, obtained from a high-precision IR-marker positioning system.

The positional RMSE per noise configuration is presented in Fig. 4. The EKF diverges for almost all process noise configurations (divergence approximately corresponds to an RMSE higher than 1 m). The IEKF and damped IEKF improve the situation somewhat but still diverge in a lot of cases. The DIEKF and damped DIEKF improve the performance even further and essentially only diverge for very low process noise tuning. As the process noise is increased, the difference between the algorithms decreases but still favors the DIEKF and damped DIEKF, showing strong robustness to the process noise tuning.

## VI. DISCUSSION & CONCLUSION

Finally, we will discuss relationships to other works and conclude the article with some future research directions.

### A. Related work

In this work, we have presented a unified framework of so-called *dynamically iterated filters* (DIFs). However, certain special cases of DIFs have been presented previously in the literature. For instance, the DIPLF first presented in [34], for the purpose of robustly estimating the process noise variance, a motivation which is completely different from ours. A similar motivation to ours appears in [36] where the L-scan IPLF is introduced. The L-scan IPLF also re-linearizes the dynamical model through an  $L$ -lag smoothing procedure. However, even in the case of  $L = 1$ , it requires access to previous measurements, something we do not consider here, as this technically makes it a smoother.

The origin of the DIEKF can be traced back to [38], where it was developed through principles of feedback, lacking a proper theoretical motivation. In contrast, we unify DIFs based on analytical and statistical linearization in a common framework. This allows for a plethora of special variants of DIFs to be developed, depending on the chosen variant of SL. As such, while we only consider the unscented transform as our choice of SL, dynamically iterated analogs of other variants of sigma-point filters are readily available by making another choice of SL. One may also note that while we do recognize the vast literature on sigma-point filters, we have limited our references to a select few representative examples.

As alluded to in Section III-D, the DIFs may also be interpreted as a one-step fixed-lag smoother. As such, the different special cases have strong connections to the IEKS [35] and the IPLS [36]. Further, the damped versions have strong connections to fixed-lag alternatives of the damped versions of the IEKS and IPLS [29], [30].

Other alternatives to nonlinear filtering are also noteworthy, such as the PF [7] and PMF [6], which are both applicable to a wider range of models than the algorithms presented here. However, these have exponential complexity in the dimension

of the state and are thus typically limited to lower-dimensional systems. If the model is restricted to contain a linear Gaussian substructure, the exponential complexity has been somewhat remedied by Rao–Blackwellized versions, such as the *Rao–Blackwellized particle filter* (RBPF) [5], [39]. Nevertheless, with a high-dimensional nonlinear evolution, the complexity remains.

## B. Summary & Conclusion

A unified framework of DIFs has been presented. Contrary to previous iterated filters, DIFs are useful for all possible combinations of (Gaussian) linear and nonlinear transition and measurement models. Further, the DIFs were shown to be GN methods and damped versions of the DIFs could thus be readily developed. The DIFs were evaluated against both their non-iterated as well as standard iterated counterparts. In all numerical examples, the DIFs showed superior performance and robustness properties. As a future research direction, it would be interesting to study the convergence properties of the DIFs as compared to regular iterated filters which should be possible through the lens of GN optimization. Further, quantifying the properties of the models that benefit from the DIF as opposed to standard filters could be interesting.

## APPENDIX

**Identity 1** (Woodbury Matrix Identity). *Assume that  $\mathbf{L}$  and  $\Sigma$  are invertible matrices. Then,*

$$\begin{aligned} (\mathbf{A}\mathbf{L}\mathbf{A}^\top + \Sigma)^{-1} &= \\ \Sigma^{-1} - \Sigma^{-1}\mathbf{A}(\mathbf{L}^{-1} + \mathbf{A}^\top\Sigma^{-1}\mathbf{A})^{-1}\mathbf{A}^\top\Sigma^{-1}. \end{aligned}$$

**Identity 2** (Kalman gain). *Assume that  $\mathbf{L}$  and  $\Sigma$  are invertible matrices. Then, by Identity 1*

$$\begin{aligned} \mathbf{L}\mathbf{A}^\top(\mathbf{A}\mathbf{L}\mathbf{A}^\top + \Sigma)^{-1} &= \\ \mathbf{L}\mathbf{A}^\top\left(\Sigma^{-1} - \Sigma^{-1}\mathbf{A}(\mathbf{L}^{-1} + \mathbf{A}^\top\Sigma^{-1}\mathbf{A})^{-1}\mathbf{A}^\top\Sigma^{-1}\right) &= \\ \underbrace{\mathbf{L}([\mathbf{L}^{-1} + \mathbf{A}^\top\Sigma^{-1}\mathbf{A}] - \mathbf{A}^\top\Sigma^{-1}\mathbf{A})}_{=I} \times & \\ [\mathbf{L}^{-1} + \mathbf{A}^\top\Sigma^{-1}\mathbf{A}]^{-1}\mathbf{A}^\top\Sigma^{-1} &= \\ [\mathbf{L}^{-1} + \mathbf{A}^\top\Sigma^{-1}\mathbf{A}]^{-1}\mathbf{A}^\top\Sigma^{-1} \end{aligned}$$

Assume a transition model and a measurement model given by

$$\mathbf{x}_{k+1} = \mathbf{f}(\mathbf{x}_k) + \mathbf{w}_k \quad (34a)$$

$$\mathbf{y}_k = \mathbf{h}(\mathbf{x}_k) + \mathbf{e}_k, \quad (34b)$$

where  $\mathbf{w}_k \sim \mathcal{N}(\mathbf{w}_k; \mathbf{0}, \mathbf{Q})$  and  $\mathbf{e}_k \sim \mathcal{N}(\mathbf{e}_k; \mathbf{0}, \mathbf{R})$  are mutually independent.

The (linearized) mean measurement update and mean smoothing step for this model are given by

$$\mathbf{x}_{k|k} = \mathbf{x}_{k|k-1} + \mathbf{K}_k(\mathbf{y}_k - \mathbf{h}(\mathbf{x}_{k|k-1})) \quad (35a)$$

$$\mathbf{x}_{k|k+1} = \mathbf{x}_{k|k} + \mathbf{G}_k(\mathbf{x}_{k+1|k+1} - \mathbf{f}(\mathbf{x}_{k|k})), \quad (35b)$$

where

$$\begin{aligned} \mathbf{H} &\triangleq \frac{d}{d\mathbf{x}}\mathbf{h}(\mathbf{x})|_{\mathbf{x}=\mathbf{x}_{k|k-1}} & \tilde{\mathbf{R}} &\triangleq \mathbf{R} + \Omega_{\mathbf{h}} \\ \mathbf{F} &\triangleq \frac{d}{d\mathbf{x}}\mathbf{f}(\mathbf{x})|_{\mathbf{x}=\mathbf{x}_{k|k}} & \tilde{\mathbf{Q}} &\triangleq \mathbf{Q} + \Omega_{\mathbf{f}}, \end{aligned}$$

where  $\Omega_{\mathbf{f}}$  and  $\Omega_{\mathbf{h}}$  are parameters of the linearization, as given by (19) or (18). Further, the gains  $\mathbf{K}_k$  and  $\mathbf{G}_k$  are given by

$$\begin{aligned} \mathbf{K}_k &\triangleq \mathbf{P}_{k|k-1}\mathbf{H}^\top \left( \mathbf{H}\mathbf{P}_{k|k-1}\mathbf{H}^\top + \tilde{\mathbf{R}} \right)^{-1} \\ &\quad \underbrace{\triangleq \Gamma}_{\left( \mathbf{P}_{k|k-1}^{-1} + \mathbf{H}^\top\tilde{\mathbf{R}}^{-1}\mathbf{H} \right)^{-1}} \mathbf{H}^\top\tilde{\mathbf{R}}^{-1} \quad (36) \\ \mathbf{G}_k &\triangleq \mathbf{P}_{k|k}\mathbf{F}^\top \left( \mathbf{F}\mathbf{P}_{k|k}\mathbf{F}^\top + \tilde{\mathbf{Q}} \right)^{-1} \\ &\quad \left( \mathbf{P}_{k|k}^{-1} + \mathbf{F}^\top\tilde{\mathbf{Q}}^{-1}\mathbf{F} \right)^{-1} \mathbf{F}^\top\tilde{\mathbf{Q}}^{-1} = \\ &\quad \underbrace{\left( \mathbf{P}_{k|k-1}^{-1} + \mathbf{H}^\top\tilde{\mathbf{R}}^{-1}\mathbf{H} + \mathbf{F}^\top\tilde{\mathbf{Q}}^{-1}\mathbf{F} \right)^{-1}}_{\triangleq \Lambda} \mathbf{F}^\top\tilde{\mathbf{Q}}^{-1}, \quad (37) \end{aligned}$$

by Identity 2.

Note that (35a) and (35b) can thus also be written as

$$\mathbf{x}_{k|k} = \mathbf{x}_{k|k-1} + \Gamma\mathbf{H}^\top\tilde{\mathbf{R}}^{-1}(\mathbf{y}_k - \mathbf{h}(\mathbf{x}_{k|k-1})) \quad (38a)$$

$$\mathbf{x}_{k|k+1} = \mathbf{x}_{k|k} + \Lambda\mathbf{F}^\top\tilde{\mathbf{Q}}^{-1}(\mathbf{x}_{k+1|k+1} - \mathbf{f}(\mathbf{x}_{k|k})). \quad (38b)$$

Using (38a) in (38b) yields

$$\begin{aligned} \mathbf{x}_{k|k+1} &= \mathbf{x}_{k|k-1} + \underbrace{\Gamma\mathbf{H}^\top\tilde{\mathbf{R}}^{-1}(\mathbf{y}_k - \mathbf{h}(\mathbf{x}_{k|k-1}))}_{(A)} + \\ &\quad \underbrace{\Lambda\mathbf{F}^\top\tilde{\mathbf{Q}}^{-1}(\mathbf{x}_{k+1|k+1} - \mathbf{f}(\mathbf{x}_{k|k}))}_{(B)}. \quad (39) \end{aligned}$$

Focusing on (B), note that

$$\begin{aligned} \mathbf{x}_{k+1|k+1} - \mathbf{f}(\mathbf{x}_{k|k}) &= \\ (\mathbf{x}_{k+1|k+1} - \mathbf{f}(\mathbf{x}_{k|k-1})) + (\mathbf{f}(\mathbf{x}_{k|k-1}) - \mathbf{f}(\mathbf{x}_{k|k})) &\approx \\ (\mathbf{x}_{k+1|k+1} - \mathbf{f}(\mathbf{x}_{k|k-1})) + & \\ (\mathbf{f}(\mathbf{x}_{k|k}) + \mathbf{F}(\mathbf{x}_{k|k-1} - \mathbf{x}_{k|k}) - \mathbf{f}(\mathbf{x}_{k|k})) &= \\ (\mathbf{x}_{k+1|k+1} - \mathbf{f}(\mathbf{x}_{k|k-1})) - \mathbf{F}\Gamma\mathbf{H}^\top\tilde{\mathbf{R}}^{-1}(\mathbf{y}_k - \mathbf{h}(\mathbf{x}_{k|k-1})), \end{aligned}$$

where the last equality comes from (38a).

Thus, (B) can be written as

$$\begin{aligned} \underbrace{\Lambda\mathbf{F}^\top\tilde{\mathbf{Q}}^{-1}(\mathbf{x}_{k+1|k+1} - \mathbf{f}(\mathbf{x}_{k|k-1}))}_{(C)} + \\ \underbrace{-\Lambda\mathbf{F}^\top\tilde{\mathbf{Q}}^{-1}\mathbf{F}\Gamma\mathbf{H}^\top\tilde{\mathbf{R}}^{-1}(\mathbf{y}_k - \mathbf{h}(\mathbf{x}_{k|k-1}))}_{(D)}. \quad (40) \end{aligned}$$

Combining (A) and (D) yields

$$\begin{aligned} \Lambda\mathbf{F}^\top\tilde{\mathbf{Q}}^{-1}\mathbf{F} \underbrace{\left[ \left( \Lambda\mathbf{F}^\top\tilde{\mathbf{Q}}^{-1}\mathbf{F} \right)^{-1} \Gamma\mathbf{H}^\top\tilde{\mathbf{R}}^{-1} - \Gamma\mathbf{H}^\top\tilde{\mathbf{R}}^{-1} \right]}_{(E)} \times \\ (\mathbf{y}_k - \mathbf{h}(\mathbf{x}_{k|k-1})). \quad (41) \end{aligned}$$

We proceed with (E) which can be simplified as

$$\begin{aligned}
& (\Lambda \mathbf{F}^\top \tilde{\mathbf{Q}}^{-1} \mathbf{F})^{-1} \Gamma \mathbf{H}^\top \tilde{\mathbf{R}}^{-1} - \Gamma \mathbf{H}^\top \tilde{\mathbf{R}}^{-1} = \\
& (\mathbf{F}^\top \tilde{\mathbf{Q}}^{-1} \mathbf{F})^{-1} \left( \mathbf{P}_{k|k-1}^{-1} + \mathbf{H}^\top \tilde{\mathbf{R}}^{-1} \mathbf{H} + \mathbf{F}^\top \tilde{\mathbf{Q}}^{-1} \mathbf{F} \right) \Gamma \mathbf{H}^\top \tilde{\mathbf{R}}^{-1} - \\
& \Gamma \mathbf{H}^\top \tilde{\mathbf{R}}^{-1} = \\
& (\mathbf{F}^\top \tilde{\mathbf{Q}}^{-1} \mathbf{F})^{-1} \overbrace{\left( \mathbf{P}_{k|k-1}^{-1} + \mathbf{H}^\top \tilde{\mathbf{R}}^{-1} \mathbf{H} \right)}{=\Gamma^{-1}} \Gamma \mathbf{H}^\top \tilde{\mathbf{R}}^{-1} = \\
& (\mathbf{F}^\top \tilde{\mathbf{Q}}^{-1} \mathbf{F})^{-1} \mathbf{H}^\top \tilde{\mathbf{R}}^{-1}.
\end{aligned}$$

Hence, (41) is given by

$$\begin{aligned}
& \Lambda \mathbf{F}^\top \tilde{\mathbf{Q}}^{-1} \mathbf{F} (\mathbf{F}^\top \tilde{\mathbf{Q}}^{-1} \mathbf{F})^{-1} \mathbf{H}^\top \tilde{\mathbf{R}}^{-1} (\mathbf{y}_k - \mathbf{h}(\mathbf{x}_{k|k-1})) = \\
& \Lambda \mathbf{H}^\top \tilde{\mathbf{R}}^{-1} (\mathbf{y}_k - \mathbf{h}(\mathbf{x}_{k|k-1})). \quad (42)
\end{aligned}$$

Thus, reinserting (C) and (42) into (39) gives

$$\begin{aligned}
\mathbf{x}_{k|k+1} &= \mathbf{x}_{k|k-1} + \Lambda \left[ \mathbf{H}^\top \tilde{\mathbf{R}}^{-1} (\mathbf{y}_k - \mathbf{h}(\mathbf{x}_{k|k-1})) + \right. \\
& \left. \mathbf{F}^\top \tilde{\mathbf{Q}}^{-1} (\mathbf{x}_{k+1|k+1} - \mathbf{f}(\mathbf{x}_{k|k-1})) \right] = \\
& \mathbf{x}_{k|k-1} + \Lambda \left[ \mathbf{H}^\top (\mathbf{R} + \mathbf{\Omega}_h)^{-1} (\mathbf{y}_k - \mathbf{h}(\mathbf{x}_{k|k-1})) + \right. \\
& \left. \mathbf{F}^\top (\mathbf{Q} + \mathbf{\Omega}_f)^{-1} (\mathbf{x}_{k+1|k+1} - \mathbf{f}(\mathbf{x}_{k|k-1})) \right]. \quad (43)
\end{aligned}$$

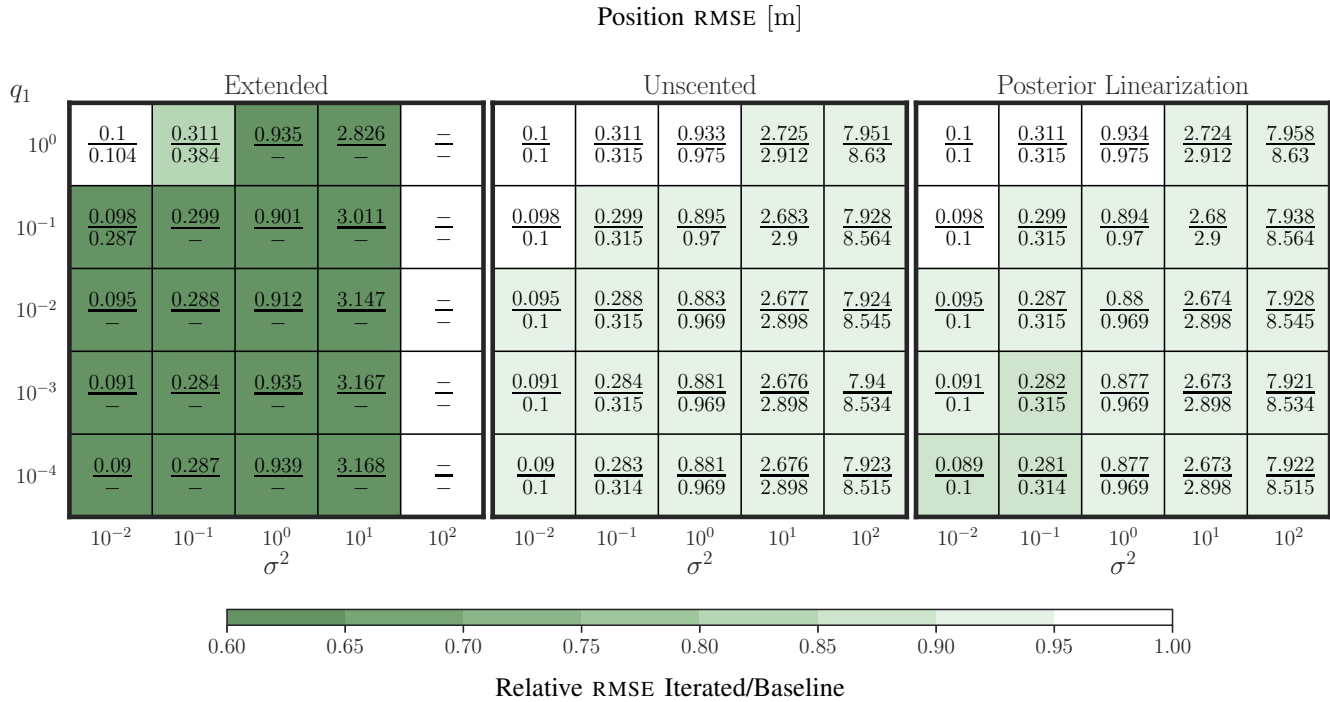
Hence, with fixed  $\mathbf{\Omega}_h$ ,  $\mathbf{\Omega}_f$ ,  $\mathbf{P}_{k-1}$  and  $\mathbf{P}_k$ , (43) is identical to the smoothing step in [35] and thus minimizes the same loss, which, for one time step, is given by

$$\begin{aligned}
\mathcal{L} &= (\mathbf{x}_{k-1} - \mathbf{x}_{k-1|k-1})^\top \mathbf{P}_{k-1|k-1}^{-1} (\mathbf{x}_{k-1} - \mathbf{x}_{k-1|k-1}) + \\
& (\mathbf{y}_k - \mathbf{h}(\mathbf{x}_k))^\top (\mathbf{R} + \mathbf{\Omega}_h)^{-1} (\mathbf{y}_k - \mathbf{h}(\mathbf{x}_k)) + \\
& (\mathbf{x}_k - \mathbf{f}(\mathbf{x}_{k-1}))^\top (\mathbf{Q} + \mathbf{\Omega}_f)^{-1} (\mathbf{x}_k - \mathbf{f}(\mathbf{x}_{k-1})). \quad (44)
\end{aligned}$$

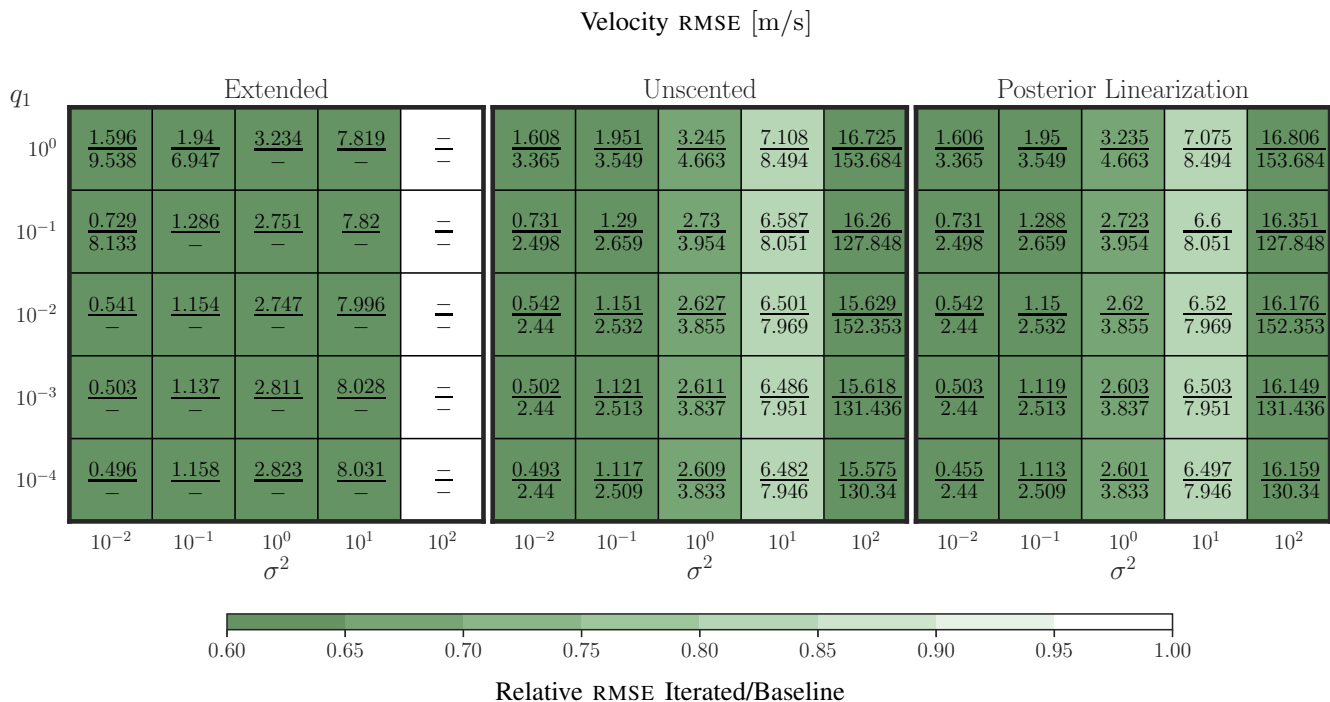
## REFERENCES

- [1] R. E. Kalman, "A New Approach to Linear Filtering and Prediction Problems," *Journal of Basic Engineering*, vol. 82, no. 1, pp. 35–45, Mar. 1960.
- [2] H. E. Rauch, F. Tung, and C. T. Striebel, "Maximum likelihood estimates of linear dynamic systems," *AIAA Journal*, vol. 3, no. 8, pp. 1445–1450, 1965.
- [3] S. Julier, J. Uhlmann, and H. Durrant-Whyte, "A New Approach for Filtering Nonlinear Systems," in *Proceedings of 1995 American Control Conference - ACC'95*, vol. 3. Seattle, WA, USA: American Autom Control Council, 1995, pp. 1628–1632.
- [4] I. Arasaratnam and S. Haykin, "Cubature Kalman Filters," *IEEE Trans. Automat. Contr.*, vol. 54, no. 6, pp. 1254–1269, Jun. 2009.
- [5] T. Schön, F. Gustafsson, and P.-J. Nordlund, "Marginalized particle filters for mixed linear/nonlinear state-space models," *IEEE Trans. Signal Process.*, vol. 53, no. 7, pp. 2279–2289, 2005.
- [6] R. Bucy and K. Senne, "Digital synthesis of non-linear filters," *Automatica*, vol. 7, no. 3, pp. 287–298, 1971.
- [7] N. Gordon, D. Salmond, and A. Smith, "Novel approach to nonlinear/non-gaussian bayesian state estimation," *IEE Proceedings F (Radar and Signal Processing)*, vol. 140, pp. 107–113(6), Apr. 1993.
- [8] H. Cox, "On the estimation of state variables and parameters for noisy dynamic systems," *IEEE Trans. Automat. Contr.*, vol. 9, no. 1, pp. 5–12, 1964.
- [9] S. Särkkä, "Unscented Rauch–Tung–Striebel Smoother," *IEEE Trans. on Automat. Contr.*, vol. 53, no. 3, pp. 845–849, Apr. 2008.
- [10] G. Kitagawa, "Monte Carlo filter and smoother for non-gaussian nonlinear state space models," *Journal of Computational and Graphical Statistics*, vol. 5, no. 1, pp. 1–25, 1996.
- [11] T. Lefebvre, H. Bruyninckx, and J. De Schuller, "Comment on "A new method for the nonlinear transformation of means and covariances in filters and estimators" [with authors' reply]," *IEEE Trans. Automat. Contr.*, vol. 47, no. 8, pp. 1406–1409, Aug. 2002.
- [12] P. Closas, C. Fernandez-Prades, and J. Vila-Valls, "Multiple Quadrature Kalman Filtering," *IEEE Trans. Signal Process.*, vol. 60, no. 12, pp. 6125–6137, Dec. 2012.
- [13] J. Steinbring and U. D. Hanebeck, "LRKF Revisited: The Smart Sampling Kalman Filter (S2KF)," *Journal of Advances in Information Fusion*, vol. 9, no. 2, 2014.
- [14] S. Wang, J. Feng, and C. K. Tse, "Spherical Simplex-Radial Cubature Kalman Filter," *IEEE Signal Process. Lett.*, vol. 21, no. 1, pp. 43–46, Jan. 2014.
- [15] J. Kotecha and P. Djuric, "Gaussian particle filtering," *IEEE Trans. Signal Process.*, vol. 51, no. 10, pp. 2592–2601, Oct. 2003.
- [16] Y. Wu, X. Hu, D. Hu, and M. Wu, "Comments on "Gaussian particle filtering,"" *IEEE Trans. Signal Process.*, vol. 53, no. 8, pp. 3350–3351, Aug. 2005.
- [17] W. Denham and S. Pines, "Sequential estimation when measurement function nonlinearity is comparable to measurement error," in *Guidance Control Conference*, ser. Guidance, Navigation, and Control and Co-located Conferences, Aug. 1965.
- [18] B. M. Bell and F. W. Cathey, "The iterated Kalman filter update as a Gauss-Newton method," *IEEE Trans. Automat. Contr.*, vol. 38, no. 2, pp. 294–297, Feb. 1993.
- [19] P. Teunissen, "On the Local Convergence of the Iterated Extended Kalman Filter," in *Proceeding of the XX General Assembly of the IUGG*, Aug. 1994.
- [20] M. A. Skoglund, F. Gustafsson, and G. Hendeby, "On Iterative Unscented Kalman Filter using Optimization," in *2019 22th International Conference on Information Fusion (FUSION)*, Ottawa, ON, Canada, Jul. 2019, pp. 1–8.
- [21] R. Zhan and J. Wan, "Iterated Unscented Kalman Filter for Passive Target Tracking," *IEEE Trans. Aerosp. Electron. Syst.*, vol. 43, no. 3, pp. 1155–1163, Jul. 2007.
- [22] Á. F. García-Fernández, L. Svensson, and M. R. Morelande, "Iterated Statistical Linear Regression for Bayesian Updates," in *17th International Conference on Information Fusion (FUSION)*, Salamanca, Spain, Jul. 2014, pp. 1–8.
- [23] Á. F. García-Fernández, L. Svensson, M. R. Morelande, and S. Särkkä, "Posterior Linearization Filter: Principles and Implementation Using Sigma Points," *IEEE Trans. Signal Process.*, vol. 63, no. 20, pp. 5561–5573, Oct. 2015.
- [24] A. H. Jazwinski, *Stochastic Processes and Filtering Theory*. Academic Press, 1970.
- [25] G. Sibley, G. Sukhatme, and L. Matthies, "The Iterated Sigma Point Kalman Filter with Applications to Long Range Stereo," in *Robotics: Science and Systems II*. Robotics: Science and Systems Foundation, Aug. 2006.
- [26] M. A. Skoglund, G. Hendeby, and D. Axehill, "Extended Kalman Filter Modifications Based on an Optimization view point," in *2015 18th International Conference on Information Fusion (Fusion)*, Jul. 2015, pp. 1856–1861.
- [27] M. Raitoharju, L. Svensson, Á. F. García-Fernández, and R. Piché, "Damped Posterior Linearization Filter," *IEEE Signal Process. Lett.*, vol. 25, no. 4, pp. 536–540, Apr. 2018.
- [28] J. Nocedal and S. Wright, *Numerical Optimization (Springer Series in Operations Research and Financial Engineering)*, 2nd ed. Springer, Jul. 2006.
- [29] S. Särkkä and L. Svensson, "Levenberg-Marquardt and Line-Search Extended Kalman Smoothers," in *ICASSP 2020 - 2020 IEEE Int. Conf. Acoust. Speech Signal Process. ICASSP*. Barcelona, Spain: IEEE, May 2020, pp. 5875–5879.
- [30] J. Lindqvist, S. Särkkä, Á. F. García-Fernández, M. Raitoharju, and L. Svensson, "Posterior Linearisation Smoothing with Robust Iterations," Dec. 2021, arXiv:2112.03969.
- [31] A. Kullberg, I. Skog, and G. Hendeby, "Iterated Filters for Nonlinear Transition Models," in *2023 26th International Conference on Information Fusion (FUSION)*, Charleston, SC, USA, Jul. 2023, pp. 1–8.
- [32] S. Särkkä, *Bayesian Filtering and Smoothing*, 1st ed. Cambridge University Press, Sep. 2013.
- [33] I. Elishakoff and S. H. Crandall, "Sixty years of stochastic linearization technique," *Meccanica*, vol. 52, no. 1-2, pp. 299–305, Jan. 2017.
- [34] M. Raitoharju, R. Hostettler, and S. Särkkä, "Posterior Linearisation Filter for Non-linear State Transformation Noises," in *2022 25th International Conference on Information Fusion (FUSION)*. Linköping, Sweden: IEEE, Jul. 2022, pp. 1–6.

- [35] B. M. Bell, "The Iterated Kalman Smoother as a Gauss–Newton Method," *SIAM J. Optim.*, vol. 4, no. 3, pp. 626–636, Aug. 1994.
- [36] Á. F. García-Fernández, L. Svensson, and S. Särkkä, "Iterated Posterior Linearization Smoother," *IEEE Trans. Automat. Contr.*, vol. 62, no. 4, pp. 2056–2063, Apr. 2017.
- [37] A. Kullberg, M. A. Skoglund, I. Skog, and G. Hendeby, "On the relationship between iterated statistical linearization and quasi-newton methods," *IEEE Signal Process. Lett.*, pp. 1–5, 2023.
- [38] R. P. Wishner, J. A. Tabaczynski, and M. Athans, "On the Estimation of the State of Noisy Nonlinear Multivariable Systems," in *IFAC Symp. Multivariable Control Syst.*, Düsseldorf, 1968.
- [39] R. Karlsson, T. Schön, and F. Gustafsson, "Complexity analysis of the marginalized particle filter," *IEEE Trans. Signal Process.*, vol. 53, no. 11, pp. 4408–4411, Nov. 2005.



(a) Position RMSE. The analytically linearized DIEKF improves the most over its baseline the EKF which diverges for 22/25 configurations. The DIUKF and DIPLF have similar performance, where the DIPLF is slightly better for some configurations.



(b) Velocity RMSE. All three DIFs have substantially better performance than their corresponding baselines. The DIEKF has 10-fold improvements and the DIUKF and DIPLF have approximately a 5-fold improvement in low noise regimes. The results are even better for the DIUKF and DIPLF in high noise regimes, with approximately 10-fold improvements.

Fig. 5: RMSE for the DIFs as compared to their respective baselines in the second numerical example. The top number in each cell is the RMSE for the DIF whereas the bottom number is the RMSE for the corresponding baseline. A “-” indicates that the position RMSE of the filter is larger than  $\sigma$  and it thus considered to have diverged. The left plot in (a) and (b) shows the RMSE for the DIEKF and EKF. The middle figure shows the DIUKF and UKF and finally, the rightmost figure shows the DIPLF and UKF. Each cell is colored according to the RMSE of the DIF relative to the baseline; the relative RMSE is simply the fraction of the RMSE.